

# Transverse Single Spin Asymmetries in Hadronic Interactions

## An Experimental Overview and Outlook

L.C. Bland

<sup>1</sup>Brookhaven National Laboratory, Upton, New York (USA)

**Abstract.** Transverse single-spin asymmetries (SSA) are expected to be small in perturbative QCD because of the chiral nature of the theory. Experiment shows there are large transverse SSA for particles produced in special kinematics. This contribution reviews the experimental situation and provides an outlook for future measurements.

### 1 Introduction

We now agree that Quantum Chromodynamics (QCD) is the theory of the strong interaction. QCD describes mesons and baryons as being composed of color-charged quarks ( $q$ ) and anti-quarks that interact via the exchange of gluons ( $g$ ). Two non-trivial aspects of QCD are that the gluons carry color charge and that color is absolutely confined into color-neutral objects. These aspects make it complicated to understand the structure of mesons and baryons, and lead to emergent phenomena that are not readily evident from the QCD Lagrangian. The quest to understand how the proton gets its spin from its constituents is one avenue to tackling the big question regarding color confinement.

Since the up and down quarks are so light and QCD is a vector gauge theory, we expect that helicity is essentially unchanged at the  $q \rightarrow qg$  vertex [1], with the probability for helicity flip being proportional to the quark mass. Transverse single-spin asymmetries (SSA) are an azimuthal modulation of particles that can be observed either from decay or via spin-dependent particle production. Transverse SSA requires helicity flip, so are expected to be small. Experiment observes large transverse SSA for particles produced via the strong interaction in particular kinematics at collision energies where the hadroproduction is described by next-to-leading order (NLO) perturbative QCD (pQCD) calculations.

Spin-orbit correlations and  $qg$  correlations are two suggestions by theory why transverse SSA are so large. Transverse momentum ( $k_T$ ) can be correlated with the spin of either the quark or hadron. This  $k_T$  can be either in the initial state [2] (Sivers effect) or in the fragmentation of partons into hadrons [3] (Collins effect). An issue for the Sivers effect is that factorization theorems have not been proven for the use of  $k_T$ -dependent distribution functions to describe inclusive particle production in hadronic interactions, except in the case of Drell-Yan production. Factorization is used for collinear calculations [4] that use  $qg$

correlators [5]. The  $qg$  correlators can appear in the initial state or in the fragmentation, but are collinear so do not involve  $k_T$ . Explicit relations between initial-state  $qg$  correlators and  $k_T$  moments of the Sivers function have been found [6]. The Sivers function is important to understand because it can provide new insight into the structure of the proton, regarding the role of orbital motion of the confined partons [7, 8], although model independent connections have not been found.

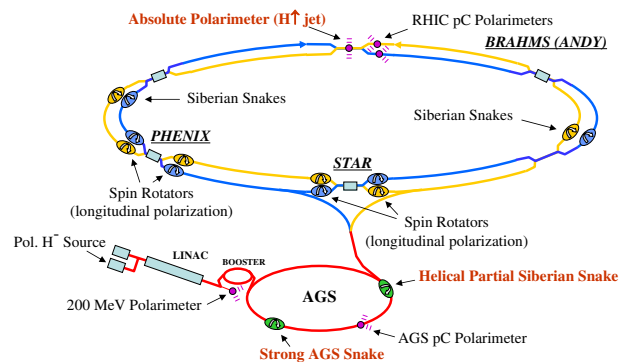


**Figure 1.** Schematic of RHIC as a polarized proton collider. Polarization is produced at the source, and is preserved through the acceleration sequence using Siberian Snake magnets. Each ring has two full snakes that each precess the polarization by  $180^\circ$ . Beams are transversely polarized in the rings. Spin rotator magnets can precess the polarization to become longitudinal at STAR and PHENIX. The 2 o'clock interaction region was originally for the BRAHMS experiment, and later for the  $A_N$ DY experiment. Results from both are discussed below.

This contribution reviews recent experimental measurements of transverse SSA in hadroproduction. Operation of the Relativistic Heavy Ion Collider (RHIC) at Brookhaven National Laboratory includes polarized proton collisions, at center-of-mass energies spanning from

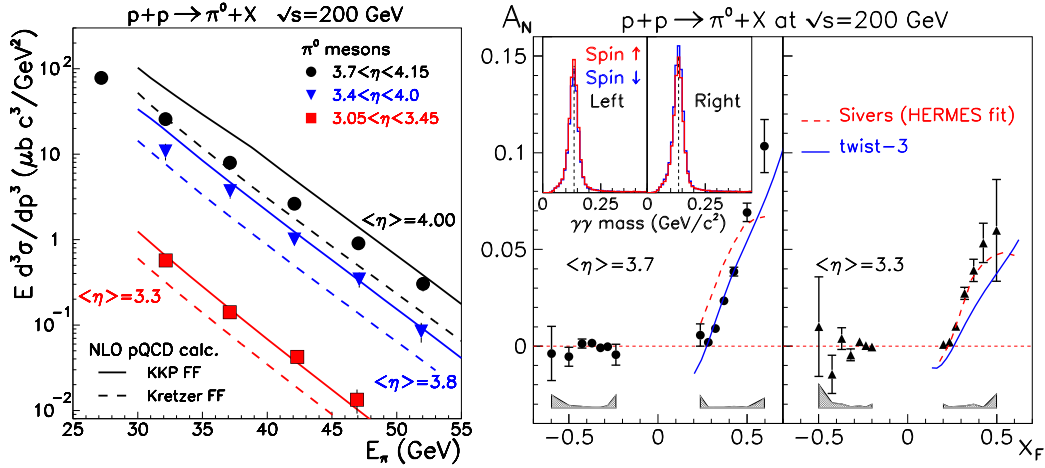


**Figure 2.** (Left) Cross sections for inclusive neutral pions produced at large  $x_F$  [15] compared to NLO pQCD calculations. (Right) Analyzing power for the inclusive production of neutral pions at large  $x_F$  [16], in comparison to calculations described in the text.

$62 < \sqrt{s} < 510$  GeV. As the first and only polarized-proton collider in the world, RHIC has provided significant new measurements of transverse SSA. Context of these new measurements is provided by reference to older measurements at fixed-target facilities that necessarily are at lower  $\sqrt{s}$ . In addition, an outlook for future measurements is provided. Theoretical understanding of these new measurements is still developing. Given that understanding emerges when experiment confronts theory, some discussion will be provided.

## 2 Transverse SSA measurements at RHIC

### 2.1 RHIC spin

Particle production at high energies typically involves accelerating ion beams most commonly done with synchrotrons. Preserving beam polarization in high-energy synchrotrons is difficult because of many intrinsic and imperfection resonances that can depolarize the beams. Collisions of high-energy polarized beams at RHIC are made possible by Siberian Snakes [9]. RHIC realizes this concept by superconducting helical dipole magnets that precess the polarization vector by  $180^\circ$  when the beam traverses the magnet, thereby resulting in perturbations of the polarization vector about the stable transverse direction as the polarized beams orbit the ring. Each RHIC ring has two Siberian Snake magnets. Similar magnets at two of the six interaction points (IP) can serve to precess transverse polarization to become longitudinal for collisions, and then restore transverse polarization after the IP. Alternatively, transversely polarized proton collisions can be studied.

It was recognized before the first polarized proton collision run that local polarimeters would be required to measure whether spin-rotator magnets were properly tuned to minimize polarization components that were transverse to the beam momenta for the colliding beams. Such local polarimeters require identifying some sort of hadroproduction from colliding beams that has non-zero

transverse SSA. Neutrons produced near  $0^\circ$  were found to have a non-zero transverse SSA [10]. The particle multiplicity observed in beam-beam counters (scintillator annuli that bracket the IP with acceptance near beam rapidity) was found to have azimuthal modulations correlated with the transverse spin. Finally, neutral pion production at large rapidity was found to have a sizeable transverse SSA [11], although the production rate is such that its use as a local polarimeter is limited. Transverse SSA are important as a tool for polarimetry. Transverse SSA have intrinsic interest, as the rest of this contribution will address.

The large RHIC experiments are at IP6 (STAR) and IP8 (PHENIX) in Fig. 1. When RHIC began, IP2 had a traditional magnetic spectrometer experiment with good particle identification (BRAHMS), with one arm viewing large rapidity particle production. More recently, a forward calorimeter experiment ( $A_N$ DY, as proposed in [12] and described in [13, 14]) was staged at IP2 for a brief time. Both BRAHMS and  $A_N$ DY made transverse SSA measurements, as discussed below. The PHENIX and STAR experiments are most heavily instrumented near midrapidity, although both experiments have implemented forward electromagnetic calorimeters that enable access to large- $x_F$  ( $x_F = 2p_L/\sqrt{s}$ , is the Feynman scaling variable) identified particle production. Forward pion detectors at STAR were made from lead glass, and viewed particles produced at  $\sim 2.5 < \eta < 4.0$  through 1-m holes in the poletips of the 0.5 T solenoid used to momentum analyze charged particles that are tracked through its time projection chamber. PHENIX implemented lead tungstate calorimeters (muon piston calorimeter) that span  $3.1 < |\eta| < 3.8$ .

Another important concept for the early RHIC spin program was the importance of measuring particle production cross sections for comparison to NLO-pQCD calculations, done concurrently with measuring spin asymmetries. A primary motivation was to ensure that the spin asymmetries were for properly reconstructed particles or ensembles. Cross section comparisons to NLO-pQCD cal-

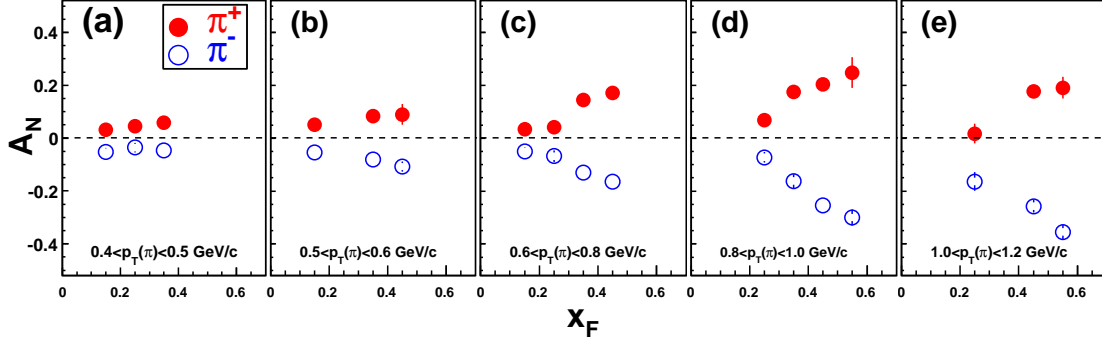


**Figure 3.** Analyzing power for  $p^\uparrow + p \rightarrow \pi^\pm + X$  at  $\sqrt{s} = 62$  GeV [18]. Large  $A_N$  is observed when the  $\pi^\pm$  are produced in the forward direction.

culations are useful to establish the applicability of theory to interpret the spin observables.

Published work to date for transverse SSA are mostly for inclusive pion production and for jets.

## 2.2 Transverse SSA for inclusive pion production

Pions are prolifically produced in high energy hadroproduction. Inclusive pion production is found [15] to have its cross section described well by NLO pQCD at RHIC energies ( $\sqrt{s} > 62$  GeV), even for pions produced in the forward direction, as defined when  $x_F$  is sizeable. There are non-zero transverse SSA for pion production [16] at large rapidity (Fig. 2), in the same kinematics where the spin-averaged cross section is in agreement with NLO pQCD. The transverse SSA for particles produced from a transversely polarized proton beam is

$$A_N = \frac{\sigma_\uparrow - \sigma_\downarrow}{\sigma_\uparrow + \sigma_\downarrow}. \quad (1)$$

This transverse SSA is called analyzing power, where  $\sigma_{\uparrow/\downarrow}$  refers to the particle production cross section for different directions of the beam polarization vector.

Operationally,  $A_N$  requires measurement of integrated luminosity for spin-up ( $\uparrow$ ) and spin-down ( $\downarrow$ ) beams. As well, the beams do not have all particles with spins pointing in a particular direction, but instead are an ensemble of particles having a polarization,  $P_{beam}$ , measured in independent counting experiments. For the data in Fig. 2, a carbon fiber was inserted into the beams at regular times for each fill and the spin dependence of recoil carbon ions was measured. The momentum transfer for the elastic scattering of polarized protons from carbon is in the region where the Coulomb amplitude for the process interferes with the nuclear amplitude. This Coulomb-Nuclear Interference (CNI) polarimeter is considered a relative polarimeter, because the spin-dependence of the nuclear amplitude is not known a priori, unlike for the Coulomb amplitude, where the spin dependence is determined from the anomalous magnetic moment of the proton. The effective normalization of the CNI polarimeter is completed by having the high-energy polarized proton beams scatter from a gas jet of hydrogen atoms, where the protons in this jet are

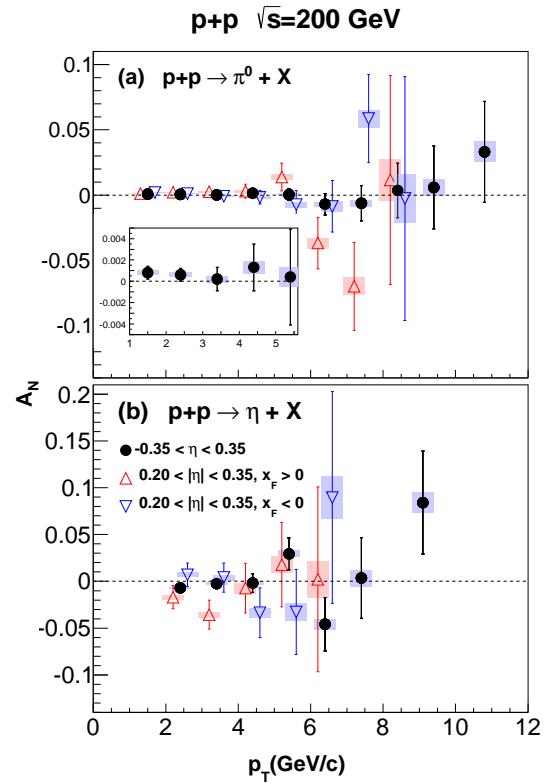


**Figure 4.** Analyzing power for  $p^\uparrow + p \rightarrow \pi^0 + X$  at  $\sqrt{s} = 200$  GeV [21]. The  $\pi^0$  are detected at midrapidity. Also shown is  $A_N$  for  $\eta \rightarrow \gamma\gamma$  reconstructed at midrapidity.

polarized [17]. Identical particle symmetries allow transfer of knowledge of the polarization of the gas jet to polarization of the proton beam. The counting rates for elastic scattering from the polarized gas jet initially required multiple fills of RHIC to get sufficient statistical precision on the beam polarization.

$A_N$  can be measured as a left/right asymmetry of the particle production from  $p^\uparrow p$  collisions in the reaction plane, defined by by the momenta of the beams and the produced particle. This left/right asymmetry can be non-zero when there is a component of the beam polarization perpendicular to the reaction plane. The convention is that

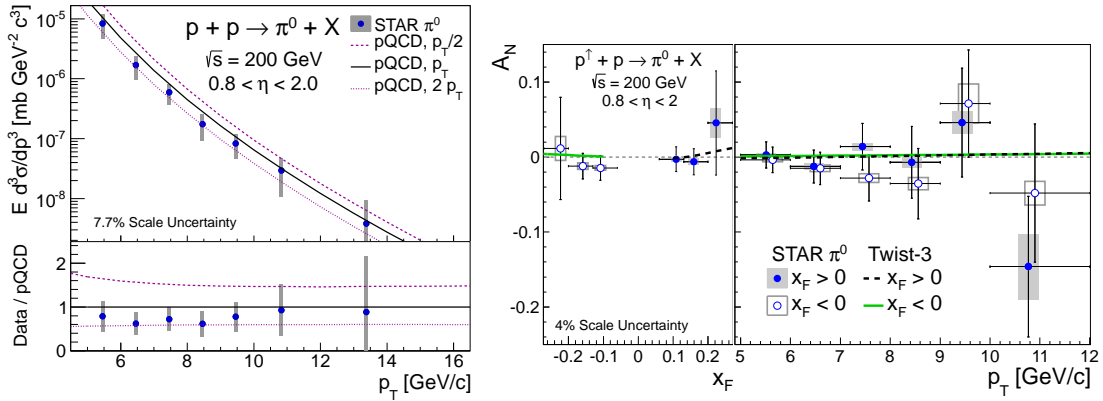


**Figure 5.** (Left) Cross sections (left) and  $A_N$  (right) for inclusive neutral pions produced at mid-central rapidity ( $0.8 < \eta < 2.0$ ) [24].

$A_N > 0$  when more particles are produced to the left when  $P_{beam}$  is up. Such a measurement requires only a single direction for the beam polarization and knowledge of the acceptance of the left and right detectors. Mirror symmetrical calorimeter modules were used for the measurements in Fig. 2. Since spin-up and spin-down polarizations were both available, operationally

$$A_N = \frac{1}{P_{beam}} \frac{\sqrt{N_{\uparrow}^L N_{\downarrow}^R} - \sqrt{N_{\downarrow}^L N_{\uparrow}^R}}{\sqrt{N_{\uparrow}^L N_{\downarrow}^R} + \sqrt{N_{\downarrow}^L N_{\uparrow}^R}}, \quad (2)$$

where  $N_{\uparrow/\downarrow}^L(R)$  refers to particle production to the left (right) of the beam whose polarization magnitude is  $P_{beam}$  pointing up ( $\uparrow$ ) or down ( $\downarrow$ ).

$A_N$  was measured for  $p^\uparrow + p \rightarrow \pi^\pm + X$  at  $\sqrt{s} = 62$  GeV [18] by the BRAHMS collaboration (Fig. 3). Charged pion production cross sections in these same kinematics were found to agree with NLO pQCD, as for neutral pion production, at  $\sqrt{s} = 200$  GeV [19]. Preliminary results show similar agreement between charged pion cross sections and NLO pQCD at  $\sqrt{s} = 62$  GeV [20]. BRAHMS was a traditional magnetic spectrometer with particle identification, so relied on concurrent measurement of spin-dependent integrated luminosities to measure  $A_N$  according to Eqn. 1.  $A_N$  at large negative  $x_F$  is also reported at  $\sqrt{s} = 62$  GeV, and found to be consistent with zero. Large positive  $A_N$  is found for  $p^\uparrow + p \rightarrow K^\pm + X$ . The large positive  $A_N$  for  $K^-$  production suggests a role played by the sea of  $q\bar{q}$  pairs within the proton, if the transverse SSA is an initial-state effect.

Inclusive  $\pi^0$  production has also been measured at mid-rapidity by the PHENIX collaboration (Fig. 4).  $A_N$  is found to be consistent with zero at mid-rapidity [21]. Particle production cross sections in these rapidity intervals are found to be consistent with NLO pQCD [23]. They also report  $A_N$  for  $\eta \rightarrow \gamma\gamma$  at midrapidity, and find it too is consistent with zero. As will be discussed below, the midrapidity measurements span the same  $p_T$  range where  $A_N(\pi^0)$  is large at large  $x_F$ .

PHENIX has implemented a forward electromagnetic calorimeter (the muon piston calorimeter). They have reported [21]  $A_N(\pi^0)$  at large  $x_F$  for  $p^\uparrow + p$  collisions at

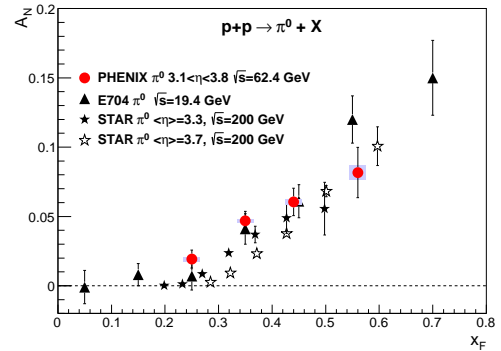


**Figure 6.** Comparison of the  $\sqrt{s}$  dependence of large- $x_F$  neutral pion production [21].

$\sqrt{s} = 62$  GeV. Their results are found to be consistent (Fig. 6) with those from Fig. 2, although at a lower  $\sqrt{s}$ . Also shown in Fig. 6 are  $A_N(\pi^0)$  measurements made by the E704 collaboration at FermiLab. E704 used a 200 GeV polarized proton beam incident on a fixed target [22]. The  $\sqrt{s}$  dependence for  $A_N$  will be discussed further below.

Neutral pion results have been reported by the STAR collaboration at rapidities intermediate between the central and forward regions ( $1 < \eta < 2$ ) [24]. As for the central and forward rapidity regions, cross sections at mid-central rapidity are consistent with NLO pQCD.  $A_N$  for neutral pion production is consistent with zero (Fig. 5) in this mid-central rapidity region.

Simple patterns are evident in the data. Spin-averaged cross sections are in agreement with NLO pQCD over a broad range of rapidity for  $\sqrt{s} > 62$  GeV. Transverse SSA are consistent with zero, except in the forward direction. A possible explanation for this is that the dynamics that gives rise to  $A_N$  involves valence quarks, that are not readily accessible at midrapidity until one reaches  $p_T > 10$  GeV/c.

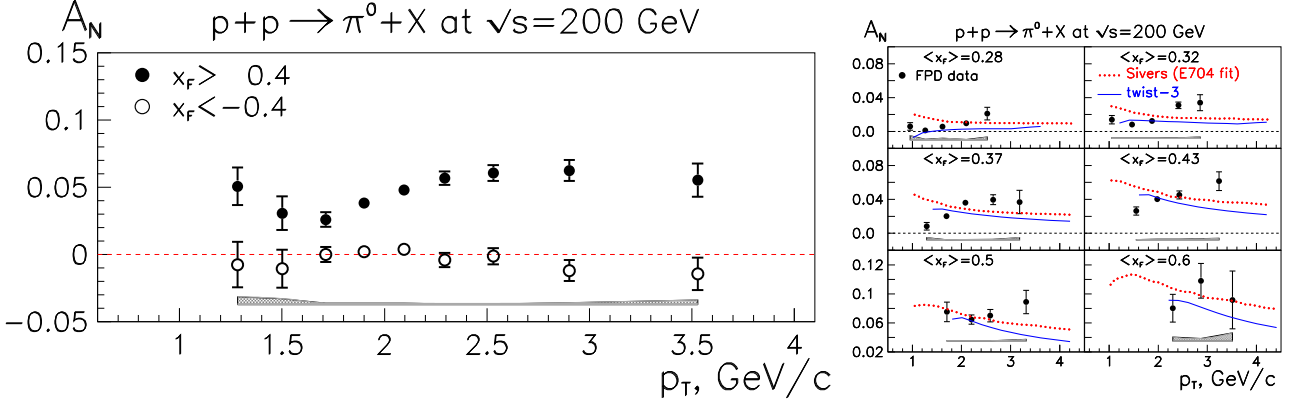


**Figure 7.** The  $p_T$  dependence of  $A_N$  for forward neutral pion production is shown. (Left)  $p_T$  dependence requiring a threshold value for  $x_F$  and (right) fully separated  $x_F$ ,  $p_T$  dependencies both show a plateau of  $A_N$  with increasing  $p_T$  [15].

### 2.3 $p_T$ dependence of transverse SSA for forward neutral pion production

In the forward region, it is possible to disentangle  $p_T$  and  $x_F$  dependences, because both longitudinal and transverse momentum components can be large. Extensions to pQCD that are model-dependent applications of TMD or application of  $qg$  correlators in a collinear framework both naively expect that  $A_N \propto 1/p_T$ , for sufficiently large  $p_T$ .

For the  $p_T$  range measured to date,  $A_N$  is found to rise with increasing  $p_T$  as it must since there is no distinction between left and right at  $p_T = 0$ . The transverse SSA stays constant at high  $p_T$ , in the range accessible by experiment (Fig. 7). Preliminary results have extended the  $p_T$  range for measurements of  $A_N$  in neutral pion production out to  $\sim 10$  GeV/c for  $p^\uparrow + p$  collisions at  $\sqrt{s} = 500$  GeV [25].

The basic form of the  $p_T$  dependence of  $A_N$  for  $p^\uparrow p \rightarrow \pi X$  is reminiscent of other transverse SSA phenomena, as measured in fixed-target experiments. Such  $p_T$  dependencies are observed for the induced polarization of hyperons in unpolarized hadroproduction: *e.g.*  $pp \rightarrow \Lambda^\uparrow X$ . When the  $\Lambda$  is produced at moderate to large  $x_F$  it has its spin preferentially (anti) aligned transverse to the production plane. At fixed  $x_F$ , the induced polarization magnitude increases with  $p_T$  to a plateau, and then persists to the highest  $p_T$  values accessible by experiment [26]. Although phenomenological treatments can explain the  $p_T$  dependence of  $p^\uparrow p \rightarrow \pi X$  [31, 32], these quantifications do not provide physical insight into this behavior.

### 2.4 Discussion

Theory has worked to explain the large transverse SSA for  $p^\uparrow + p \rightarrow \pi + X$  in the forward direction. Those explanations are constrained by measurements of transverse SSA in semi-inclusive deep inelastic scattering (SIDIS) for both the Siversons [33, 34] and Collins effects [35, 36], and in  $e^+e^-$  collisions for the Collins effect [37]. Questions about factorization in SIDIS and  $e^+e^-$  collisions have been settled. Factorized forms for these transverse SSA exist despite the presence of final-state interactions in SIDIS that are required by gauge invariance, and are required for there to

be transverse SSA. Factorized forms also exist for Drell-Yan (DY) production via  $p^\uparrow p \rightarrow \gamma^* X$ , or for generalized DY production of vector gauge bosons. For DY production, theory predicts the Siversons function will change sign relative to SIDIS because the attractive final-state interaction in the latter [38] become a repulsive initial-state interaction in the former [39]. As will be discussed below, this prediction awaits an experimental test. Complications for  $p^\uparrow p \rightarrow \pi X$  are that a mix of initial-state and final-state interactions are in general possible and that factorization for TMD distribution functions has not been proved.

One theoretical approach has been to proceed with use of TMD distribution and fragmentation functions, despite not having proven factorization for the hadroproduction of hadrons. This approach will be called generalized parton model (GPM) phenomenology in the following discussion. Another approach has been to do phenomenology using  $qg$  correlators, in a collinear twist-3 factorized framework. It was generally accepted in the community that the *soft-gluon pole* correlator was dominant. This correlator is related to the  $k_T$  moment of the Siversons function [6].

A fundamental difficulty is that TMD distribution and fragmentation functions are objects with two scales. In SIDIS, these two scales are the virtuality of the photon ( $Q^2$ ) and the transverse momentum of the observed hadron ( $p_T$ ). For  $p^\uparrow p \rightarrow \pi X$  there is only a single scale, given by the  $p_T$  of the observed  $\pi$ . This single scale does not provide access to either the magnitude of the TMD transverse momentum ( $k_T$ ) or to whether it acts in the initial-state (via the Siversons effect) or the final-state (via the Collins effect).

Theoretical calculations in Fig. 2 are GPM calculations [40] that fit Siversons moments in SIDIS [33, 34] and twist-3 calculations that use initial-state  $qg$  correlators and soft-gluon pole dominance, fitted to  $p^\uparrow p \rightarrow \pi X$  data only [41]. Compatibility of calculations of  $p^\uparrow p \rightarrow \pi X$  in the twist-3 approach and extractions of the Siversons function from SIDIS has been examined. Because of the expected dominance of initial-state interactions for  $p^\uparrow p \rightarrow \pi X$ ,  $A_N$  is found to be opposite in sign to that of the transverse SSA for SIDIS [42], using initial-state  $qg$  correlators and the

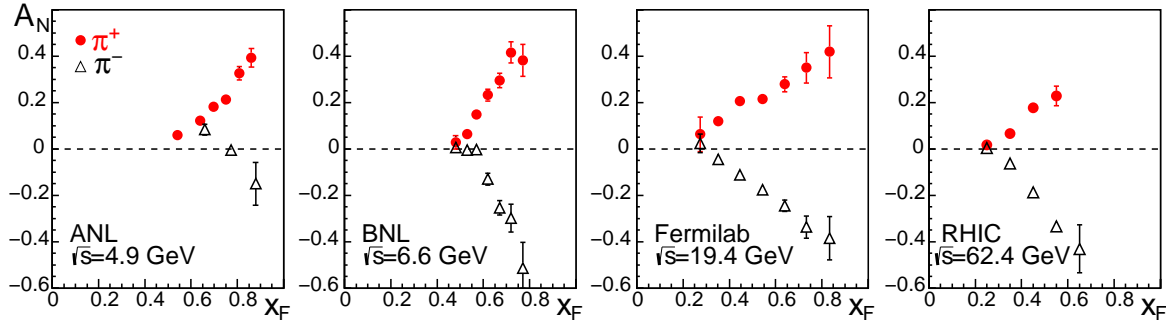


**Figure 8.**  $A_N$  for  $p^\uparrow p \rightarrow \pi^\pm X$  showing that the characteristic  $x_F$  dependence spans a broad range of  $\sqrt{s}$ , from [27] and measurements from [18, 28–30].

relation to moments of the Sivers function [6]. This sign mismatch has prompted speculations that the Sivers function may have a node. Another solution was presented at this workshop [43]. Namely, the initial expectation that the *soft-gluon pole* dominates for  $p^\uparrow p \rightarrow \pi X$  is no longer considered valid [32, 44]. A  $qg$  correlator in fragmentation, that is not related via a  $k_T$  moment to the Collins function, is now believed to be the dominant contribution to  $A_N$ . Phenomenology in this new ansatz can provide a global explanation of SIDIS and  $p^\uparrow p \rightarrow \pi X$  data. Sivers contributions are still found by twist-3 phenomenology, but they are smaller than initial estimates. The *soft-gluon pole*  $qg$  correlators are now negative, thereby cancelling large positive contributions to  $A_N$  from  $qg$  correlators in fragmentation.

GPM phenomenology still expects that the Sivers effect dominates  $A_N$  from  $p^\uparrow p \rightarrow \pi X$ . The issue for the GPM remains factorization, as the proponents have pointed out.

No theory to date provides an explanation for the persistence of transverse SSA in  $p^\uparrow p \rightarrow \pi^\pm X$  over a very broad range of  $\sqrt{s}$  (Fig. 8). The transverse SSA at  $\sqrt{s} < 20$  GeV most likely requires an explanation in terms of mesons and baryons.

It would also be interesting to see the prediction for the Collins angle distribution of the transverse SSA for a  $\pi^0$  within a jet for the final-state twist-3  $qg$  correlator now thought to be the dominant contribution to  $A_N$  for  $p^\uparrow p \rightarrow \pi X$ . There are preliminary data [45], that still require determination of the jet-energy scale, that show no dependence of the transverse SSA on the Collins angle. Determination of the jet axis and measurement of the spin-correlated azimuthal modulation of the  $\pi$  yield about this axis is expected to have small Collins contributions within the GPM [46]. Azimuthal modulations of the  $\pi$  yield within the jet is a two-scale problem analogous to SIDIS, in that the jet  $p_T$  and the pion  $k_T$  within the jet are both measured.

The question then is *where does this leave us?* I think the answer is that  $p^\uparrow p \rightarrow \pi X$  has stimulated the community to understand why such large transverse SSA exist, despite the chiral properties of QCD. Consequently, we are on the cusp of having a much richer understanding of the structure of the proton, which remains the quest. To test

that understanding, transverse SSA in  $p^\uparrow p$  are important to establish a form of *universality* of the phenomena. The task at hand for  $p^\uparrow p$  collisions is to go beyond inclusive  $\pi$  production to jets, direct photons and DY production. In the remainder of this contribution, these first steps are discussed. An outlook to the future is then provided.

## 2.5 Transverse SSA for inclusive jet production

Operations of RHIC for polarized proton collisions at  $\sqrt{s} = 500$  GeV were even more challenging than operations at  $\sqrt{s} = 200$  GeV, because of the requirements on the accelerator to preserve polarization to higher beam energies. The primary focus of  $\sqrt{s} = 500$  GeV collisions was to measure the parity-violating, longitudinal single-spin asymmetry for the production of  $W^\pm$  bosons. A proposal was put forth [12] to concurrently pursue first measurement of  $A_N$  for forward DY production to test the sign-change prediction. The first stage of the apparatus required for that measurement was staged at IP 2, in the hall originally used by the BRAHMS collaboration. That first stage apparatus used left/right symmetric hadron calorimeter modules, as shown in Fig. 9 The apparatus was ideal for measurements of  $p^\uparrow p \rightarrow \text{jet}+X$ , as discussed below.

There are many preconceptions about forward hadroproduction, and extensions from inclusive  $\pi$  production to jets immediately raises the question about what we mean by jets. To a theorist, a jet is a scattered parton. Factorized approaches ignore the couplings of hard-scattered partons to spectator partons that are required by gauge invariance, by the definition of factorization. In models, such as the string model, these couplings give rise to initial-state and final-state parton showers which also serve to complicate the definition of a jet. Despite these complexities, we proceed.

A jet is operationally defined as a pattern of energy deposition in a localized region of  $\eta - \phi$  space. Multiple algorithms exist to recognize such patterns. The favored algorithm is the anti- $k_T$  method [48], where all pairings of granular objects in  $\eta - \phi$  space are considered in the construction of a jet pattern. The granularity in this case is provided by the cells in the hadron calorimeter. We use  $R = 0.7$  for the jet finding, corresponding to the jet-cone

IP2/DY-Run11

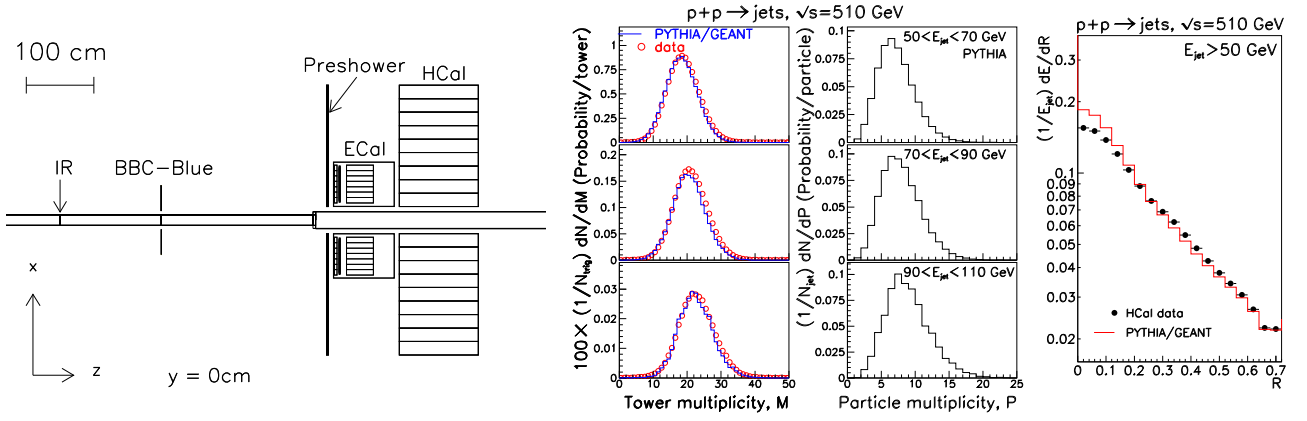


**Figure 9.** (left) Schematic of apparatus used for  $p^{\dagger}p \rightarrow \text{jet}+X$  [47]; (middle) multiplicities from the anti- $k_T$  jet-finding algorithm for (left panel) the HCal response in data and full simulation and (right panel) for particles as generated by PYTHIA [53]; (right) distribution of energy with respect to jet axis.

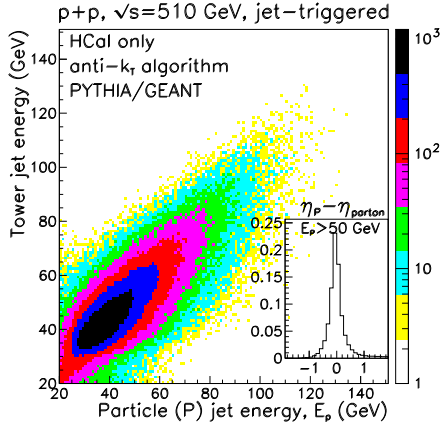


**Figure 10.** Comparison of results from the anti- $k_T$  algorithm applied to full PYTHIA + GEANT simulations versus events generated by PYTHIA [53]. The inset shows the directional match between particle jets and hard-scattered partons, and results in an 82% match when  $|\Delta\eta|, |\Delta\phi| < 0.8$ .

radius in  $\eta - \phi$  space. The mid-point cone jet finder has also been used, with similar results [49].

The result from applying the anti- $k_T$  algorithm to the calibrated response of the modular calorimeters is an object that coincides with our understanding of a jet (Fig. 9), albeit with less particle multiplicity than is observed at mid rapidity because the transverse momentum of the jet is small and  $p_T$  is generally taken as the scaling variable for QCD treatments. Forward jets have multiplicities that match those from jet studies in  $pp$  collisions in fixed target experiments [50]. The distribution of energy as a function of the distance from the jet axis in  $\eta - \phi$  space coincides with our expectations of what a jet should look like.

One note here: calibrating the response of the calorimeters is the essential and non-trivial step. The calibrations are done by applying particle finding algorithms, as described elsewhere [51]. Both electromagnetic and hadronic responses have been calibrated. The

reconstructed jets are compared against particle jets reconstructed from PYTHIA (Fig. 10).

Jet finding integrates over hadronic fragments. There are at least two significant implications: non-zero transverse SSA can only arise from initial-state spin-correlated  $k_T$  or initial-state  $qg$  correlations and given the mirror symmetry ( $A_N(\pi^+) \approx -A_N(\pi^-)$ ), the naive expectation is that the analyzing power for jets should be small.

Results for the forward jet cross section and  $A_N$  are shown in Fig. 11. Cross sections are found to be in fair agreement with NLO pQCD calculations [52], as for forward  $\pi$  production at  $\sqrt{s} > 62$  GeV. Also shown are comparisons to particle-jet results from two versions of PYTHIA. PYTHIA 6.222 [53] is the last version prior to tunings to explain underlying event contributions for midrapidity particle production at the Tevatron and PYTHIA 6.425 [54] includes first tunings, as done for preparation for the LHC. Forward particle production was not a criteria for tunings that were made, and was impacted by those tunings. This is particularly relevant for QCD backgrounds to forward DY production, discussed below.

The forward jet  $A_N$  is non-zero for  $x_F > 0$ . Collins contributions are not present, to the extent that the jet finding integrates over all fragments, as suggested it does from comparisons of particle jet results to hard scattered partons (Fig. 10). Consequently, in the TMD framework,  $A_N$  for forward jet production arises only from the Siverson effect. The anticipated cancellation of  $\pi^+$  and  $\pi^-$  contributions is observed, in that the magnitude of the jet  $A_N$  is small. Comparisons to theory that fit the Siverson function deduced from SIDIS are shown in Fig. 11. The generalized parton model (GPM) assumes factorization, and uses the Siverson function from SIDIS directly in their calculation [31]. Error bands on the calculation reflect uncertainties in the Siverson functions from SIDIS. The twist-3 calculation uses soft-gluon pole  $qg$  correlators constrained to  $k_T$  moments of the Siverson function [55]. This calculation has been cited as evidence of the color-charge reinteractions that give rise to the predicted sign change from SIDIS to DY.

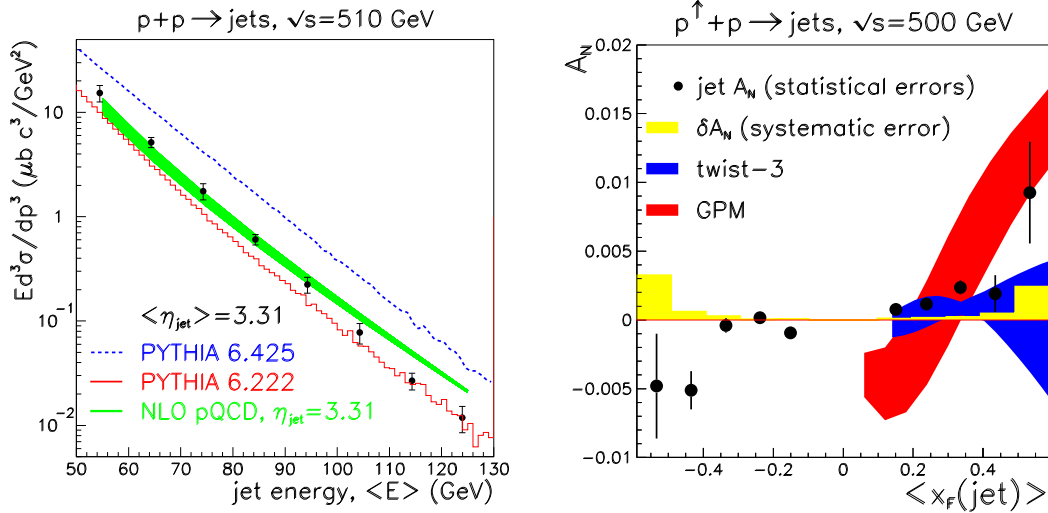


**Figure 11.** (left) Cross section for forward jet production in  $pp$  collisions at  $\sqrt{s} = 510$  GeV, in comparison to NLO pQCD and PYTHIA; (right)  $A_N$  for forward jet production, in comparison to calculations that fit the Siverts effect for SIDIS.

Mention should be made of  $A_N$  for  $x_F < 0$ . The  $p^\uparrow p \rightarrow \pi X$  results generally have  $A_N$  consistent with zero at negative  $x_F$ . The jet  $A_N$  does have a negative analyzing power with a  $\sim 3.5$  sigma significance at  $x_F \approx -0.4$ . As we heard at this workshop [56], tri-gluon correlators do predict negative analyzing power for jet production at large negative  $x_F$ . For the forward jet production, the beam with  $p_z$  opposite to that of the detected jet is a source of low- $x$  partons, in a conventional  $2 \rightarrow 2$  partonic scattering picture for the particle production. That same picture requires that partons from the  $p_z < 0$  proton have a broad distribution in  $x$ . Forward dijets select the low- $x$  component of that distribution, so could be of interest to further probe tri-gluon correlator contributions.

On the topic of jets, there are two notes of caution. Jet-finding algorithms can be applied to any detector response in a given  $\eta - \phi$  acceptance. I think we should be careful with our language, in that not all clusters of energy deposition are jets. Jets should be clustered energy depositions that are related back to the momentum of scattered partons. Absent that connection, it is difficult to relate an experimental observable to an object treated by theory. The second caution is in regard to trigger bias, and its impact on reconstructed jets. An example of this was obtained from the apparatus in Fig. 9. That apparatus was the first stage of what was to become an experiment that would measure spin observables for DY production [12]. As such, there were small electromagnetic calorimeter (ECal) modules. The ECal modules were used to trigger (via a sum of ADC values from all cells of each ECal module, corresponding after final calibrations to  $\sum E_{ECal} \geq 22$  GeV) readout for a small sample of events obtained in  $p^\uparrow p$  collisions at  $\sqrt{s} = 500$  GeV. Jets from that data sample were reconstructed and compared to jets reconstructed from HCal-triggered readout. Tower-multiplicity distributions are shown in Fig. 12. Evident in that figure is that jets triggered by the ECal modules bias the fragmentation.

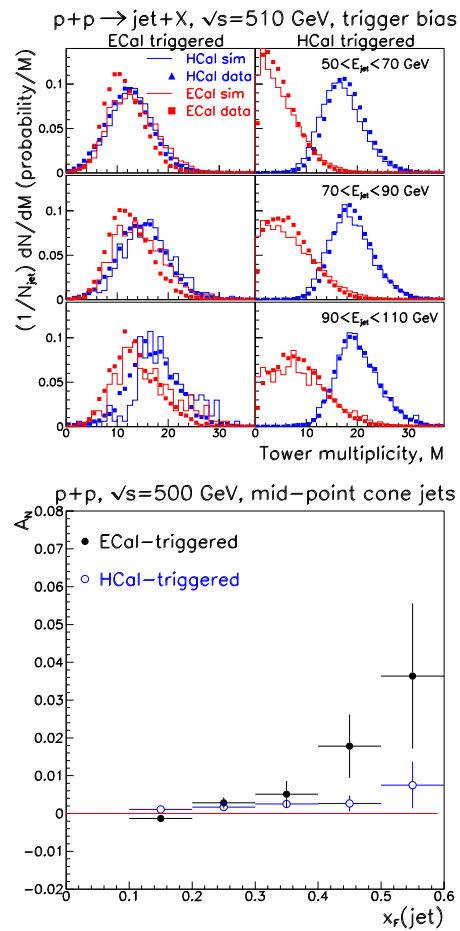


**Figure 12.** The impact of trigger bias is evident for mid-point cone jets reconstructed for events with an ECal trigger, corresponding to  $\sum E_{ECal} \geq 22$  GeV. (Top) tower multiplicity distributions show a bias towards jets with larger electromagnetic multiplicities for an ECal trigger; and (Bottom) the trigger bias makes jets more  $\pi^0$  like, thereby impacting their spin asymmetry.

The bias extends well beyond the  $\approx 22$  GeV ECal-trigger threshold. Comparing transverse SSA in the right panel of the figure shows that the bias impacts the spin observable, most likely because the jets include high-energy neutral pions as selected by the ECal-trigger.

### 3 Conclusions and Outlook

My conclusions will be brief and my outlook will be long, because there remains much to learn from  $p^\uparrow p$  collisions at RHIC.

In conclusion, RHIC has clearly demonstrated that  $p^\uparrow p \rightarrow \pi X$  with large  $x_F$  has large transverse single spin asymmetries at very high collision energies. Small and positive  $A_N$  is measured for forward jet production, in similar kinematics. Unpolarized  $\pi$  and jet cross sections are in agreement with NLO pQCD in the same kinematics, consistent with a partonic scattering origin to the spin effects. Most aspects of the measurements can be accounted for by theory, and suggest a role played by the Sivers effect.

The concurrence of the RHIC results with measurements of transverse SSA in SIDIS has led to a significant change in how we view the structure of the proton. The ideas for the importance of spin-orbit correlations that were introduced to explain large transverse SSA in  $p^\uparrow p \rightarrow \pi X$  at lower  $\sqrt{s}$  have been fully developed. Phenomenology now talks about orbiting partons as potentially an important contribution to the spin of the proton, although much work remains to prove this.

There is a consensus that polarized Drell-Yan production ( $p^\uparrow p \rightarrow \gamma^* X$  and  $\pi p^\uparrow \rightarrow \gamma^* X$ ) is a critical experiment to test a theoretical prediction that the Sivers function changes sign for polarized DY relative to SIDIS. The COMPASS collaboration will begin a polarized DY experiment later this year [57]. There are proposals to pursue polarized DY production at many laboratories, as also described at this workshop [58]. RHIC remains the only facility with polarized proton beams, and remains the world's first and only polarized proton collider. It is natural to exploit this uniqueness to address the physics question regarding the sign change of the Sivers function. The issues to be aware of include the precision to which we presently know the Sivers function from SIDIS and whether we have sufficient understanding of how the Sivers function evolves with resolution scale. Most polarized DY measurements will require  $M_{\gamma^*} > 4$  GeV/c<sup>2</sup> (as set by background considerations), corresponding to a resolution scale of 16 GeV<sup>2</sup>, whereas the SIDIS measurements have  $\langle Q^2 \rangle \approx 2.4$  GeV<sup>2</sup> [33] and 3.8 GeV<sup>2</sup> [34].

To meet the requirements for a robust test of the theoretical prediction at RHIC, forward detection of dileptons from polarized DY production is essential, so as to match the kinematics of SIDIS as closely as possible. The forward produced virtual photon should have  $0.02 \leq x_{F,\gamma^*} \leq 0.3$ , since in the forward region  $x_{F,\gamma^*}$  is to a very good approximation the Bjorken  $x$  of the quark from the polarized proton. The  $\bar{q}$  from the polarized proton has Bjorken  $x_2 \approx M_{\gamma^*}^2 / (x_{F,\gamma^*} s)$ , to a very good approximation. The  $\sqrt{s} = 500$  GeV collision energy means  $x_2 \approx 2 \times 10^{-4}$  for

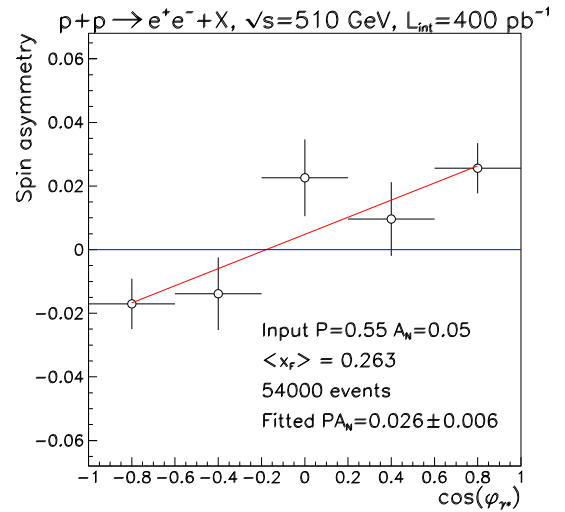


**Figure 13.** Projected sensitivity to  $A_N$  for DY production for a forward detection system proposed for installation at STAR in 2016.  $M_{\gamma^*} > 4$  GeV/c<sup>2</sup> is imposed, but otherwise DY kinematics match those from SIDIS [35, 36].

$M_{\gamma^*}=4$  GeV and  $x_{F,\gamma^*}=0.3$ . The high energy of the collider results in large partonic luminosity, to partly overcome the nucleon-nucleon luminosity advantage of fixed-target experiments. Estimates of backgrounds were made for a forward calorimeter system with tracking detectors that would observe  $e^+e^-$  dileptons from the virtual photon, with the conclusion that backgrounds can be reduced to  $< 10\%$  of the virtual photon signal. The measurement consists of  $e/\gamma$ /hadron discrimination by differences of their interactions in matter, as they shower in a calorimeter system. A preshower detector before an electromagnetic calorimeter (ECal) and a hadron calorimeter after the ECal are the primary tools to suppress backgrounds. The proposal to make this a specific experiment at IP2 at RHIC was not implemented, so that the interaction region could be used for a coherent electron cooling experiment.

There is a proposal to implement this concept at STAR, as described at this workshop [59]. That proposal includes design and construction of new forward calorimetry, so likely would not be available for a polarized DY experiment prior to 2020.

An implementation of the concept developed for the dedicated experiment can be made at STAR for 2016, using an existing calorimeter that could be modified to provide an ECal as the primary tool to detect di-electrons and an HCal behind it to reject backgrounds. As had been proposed, this calorimeter system would include a preshower detector (whose construction is underway) and tracking detectors. A test of this calorimeter was done in the 2014 RHIC run, which included  $^3\text{He}+\text{Au}$  collisions at  $\sqrt{s_{NN}} = 200$  GeV. The calorimeter proved to be robust against challenging beam conditions, as is a requirement for  $p^\uparrow p \rightarrow \gamma^* X$ . Lead glass operated during the earlier  $W$  physics program was badly discolored by radiation damage, so does not appear suitable for a forward DY experi-

ment. The bottom line is that a path exists for a polarized DY experiment to begin at STAR in 2016. Many steps remain before this path is approved and a forward DY experiment at STAR is completed. Projected statistical uncertainty for measuring  $A_N$  for forward DY production is shown in Fig. 13. The kinematics is chosen to match those of SIDIS, except that  $M_{\gamma^*} > 4 \text{ GeV}/c^2$ .

Since forward DY may be pursued with a calorimetric apparatus, there are other tantalizing prospects for transverse spin physics on the horizon. Most notably, is jet physics, where  $\pi^0$  within the jet can be accessed. A robust measurement can help to establish the fragmentation contribution to  $p^\uparrow p \rightarrow \pi X$ . In addition, the calorimetric system for polarized DY in the forward direction looks promising for reconstruction of  $\Lambda$  [51], although discrimination of  $\bar{\Lambda}$  is difficult. This opens the prospects for a measurement of induced polarization at large  $x_F$  and for a measurement of polarization transfer ( $D_{NN}$ ) for  $p^\uparrow p \rightarrow \Lambda^\uparrow X$  at  $\sqrt{s} = 500 \text{ GeV}$ .

A bright future for continued polarized proton operations at RHIC is on the horizon. Realization of that future is the goal.

## Acknowledgements

Many people have been involved in the RHIC-spin program. Special thanks to the Collider-Accelerator department, the STAR collaboration and the  $A_N$ DY collaboration. I am extremely grateful for my close collaboration with H.J. Crawford, J. Engelage, A. Ogawa, and L. Nogach.

## References

- [1] G.L. Kane, J. Pumplin, W. Repko, Phys. Rev. Lett. **41**, 1689 (1978).
- [2] D. Sivers, Phys. Rev. **D41**, 83 (1990); **D43**, 261 (1991).
- [3] J. Collins, Nucl. Phys. B **396**, 161 (1993).
- [4] J. Qiu and G.F. Sterman, Phys. Rev. Lett **67**, 2264 (1991); Nucl. Phys. B **378**, 52 (1992); Phys. Rev. **D59**, 014004 (1998).
- [5] A.V. Efremov and O.V. Teryaev, Sov. J. Nucl. Phys. **36**, 140 (1982).
- [6] X. Ji, J.-W. Qiu, W. Vogelsang, F. Yuan, Phys. Rev. Lett. **97**, 082002 (2006).
- [7] M. Burkardt, G. Schnell, Phys. Rev. D **74**, 013002 (2006).
- [8] A. Bacchetta, M. Radici, Phys. Rev. Lett. **107**, 212001 (2011).
- [9] Ya. S. Derbenev *et al.*, Part. Accel. **8**, 115 (1978).
- [10] Y. Fukao *et al.*, Phys. Lett. **B650**, 325 (2007).
- [11] J. Adams *et al.* (STAR), Phys. Rev. Lett. **92**, 171801 (2004).
- [12] *Large Rapidity Drell Yan Production at RHIC*, E.C. Aschenauer *et al.* ( $A_N$ DY), proposal to the 2011 BNL Program Advisory Committee ([http://www.bnl.gov/npp/docs/pac0611/DY\\_pro\\_110516\\_final.2.pdf](http://www.bnl.gov/npp/docs/pac0611/DY_pro_110516_final.2.pdf)).
- [13] L.Nogach *et al.* ( $A_N$ DY), *Proceedings of Dubna SPIN2011* [arXiv:1112.1812].
- [14] C. Perkins, *Proceedings of DIS2011* [arXiv:1109.0650].
- [15] J. Adams *et al.* (STAR), Phys. Rev. Lett. **97**, 152302 (2006).
- [16] B.I. Abelev *et al.* (STAR), Phys. Rev. Lett. **101**, 222001 (2008).
- [17] H. Okada *et al.*, Phys. Lett. **B638**, 450 (2006).
- [18] I. Arsene *et al.* (BRAHMS), Phys. Rev. Lett. **101**, 042001 (2008).
- [19] I. Arsene *et al.* (BRAHMS), Phys. Rev. Lett. **98**, 252001 (2007).
- [20] F. Videbaek (for BRAHMS), *Proceedings of the 23<sup>rd</sup> Winter Workshop on Nuclear Dynamics* (2007) [arXiv:0801.1696].
- [21] A. Adare *et al.* (PHENIX), submitted for publication [arXiv:1312.1995].
- [22] D.L. Adams *et al.* (E704/E581), Phys. Lett. **B261**, 201 (1991).
- [23] S.S. Adler *et al.* (PHENIX), Phys. Rev. Lett. **91**, 241803 (2003). A. Adare *et al.* (PHENIX), Phys. Rev. D **76**, 051106 (2007).
- [24] L. Adamczyk *et al.* (STAR), Phys. Rev. D **89**, 012001 (2014).
- [25] S. Heppelmann (for STAR), *Proceedings of XXI International Workshop on Deep Inelastic Scattering*, PoS DIS 2013, 240 (2013).
- [26] B. Lundberg *et al.*, Phys. Rev. D **40**, 3557 (1989).
- [27] C.A. Aidala, S.D. Bass, D. Hasch, G.K. Mallot, Rev. Mod. Phys. **85**, 655 (2013).
- [28] R.D. Klem *et al.*, Phys. Rev. Lett. **36**, 929 (1976).
- [29] C.E. Allgower *et al.*, Phys. Rev. D **65**, 092008 (2002).
- [30] D.L. Adams *et al.*, Phys. Lett. **B264**, 462 (1991).
- [31] M. Anselmino *et al.*, Phys. Rev. D **88**, 054023 (2013).
- [32] K. Kanazawa, Y. Koike, A. Metz, D. Pitonyak, Phys. Rev. D **89**, (2014).
- [33] A. Airapetian *et al.* (HERMES), Phys. Rev. Lett. **103**, 152002 (2009)
- [34] C. Adolph *et al.* (COMPASS), Phys. Lett. **B717**, 376 (2012)
- [35] A. Airapetian *et al.* (HERMES), Phys. Rev. Lett. **94**, 012002 (2005).
- [36] C. Adolph *et al.* (COMPASS), Phys. Lett. **B717**, 383 (2012).
- [37] R. Seidl *et al.* (Belle), Phys. Rev. D **78**, 032011 (2008); Phys. Rev. Lett. **96**, 232002 (2006).
- [38] S.J. Brodsky, D.S. Hwang, I. Schmidt, Phys. Lett. **B530**, 99 (2002).
- [39] J.C. Collins, Phys. Lett. **B536**, 43 (2002).
- [40] M. Boglione, U. D'Alesio, F. Murgia, Phys. Rev. D **77**, 051502 (2008).
- [41] C. Kouvaris, J. Qiu, W. Vogelsang, F. Yuan, Phys. Rev. D **74**, 114013 (2006).

- [42] Z. Kang, J. Qiu, W. Vogelsang, F. Yuan, Phys. Rev. D **83**, 094001 (2011).
- [43] D. Pitonyak, *in these proceedings* (2014).
- [44] A. Metz, D. Pitonyak, Phys. Lett. **B723**, (2013).
- [45] N. Poljak (for STAR), *Proceedings of Transversity 2011* [arXiv:1111.0755].
- [46] U. D'Alesio, F. Murgia, C. Pisano, submitted for publication [arXiv:1307.4880].
- [47] L.C. Bland *et al.* (AnDY), submitted for publication [arXiv:1304.1454].
- [48] M. Cacciari, G.P. Salam, G. Soyez, JHEP **0804**, 063 (2008).
- [49] L. Nogach (for A<sub>N</sub>DY), *Proceedings of SPIN 2012* [arXiv:1212.3437].
- [50] C. Bromberg *et al.*, Phys. Rev. Lett. **38**, 1447 (1977); M.D. Corcoran *et al.*, Phys. Rev. Lett. **41**, 9 (1978); **44**, 514 (1980); M.W. Arenton *et al.*, Phys. Rev. D **31**, 984 (1985).
- [51] L.C. Bland (for A<sub>N</sub>DY), *Proceedings of the QCD Evolution Workshop* (2013) [arXiv:1308.4705].
- [52] A. Mukerjee, W. Vogelsang, Phys. Rev. D **86**, 094009 (2012).
- [53] T. Sjöstrand *et al.*, Computer Physics Commun. **135**, 238 (2001).
- [54] T. Sjöstrand, S. Mrenna, P. Skands, JHEP **05**, 026 (2006).
- [55] L. Gamberg, Z. Kang, A. Prokudin, Phys. Rev. Lett. **110**, 232301 (2013).
- [56] Y. Koike, *in these proceedings* (2014).
- [57] M. Chiosso (for COMPASS), *in these proceedings* (2014).
- [58] J.C. Peng, *in these proceedings* (2014).
- [59] A. Vossen (for STAR), *in these proceedings* (2014).